relation functional proposed by Perdew, Burke, and Ernzerhof (PBE) [20] was adopted. To account for the valence–core interaction, ultrasoft pseudopotentials [21] were chosen for Nb 4p and 4d states and norm-conserving pseudopotentials [22] were chosen for other states. The wavefunctions were expanded in the plane-wave basis set with an energy cut-off of 25 Ry; the energy cut-off for the augmentation charge was 400 Ry. The Brillouin zone of the supercell was sampled only at the Γ point. In the energy optimization, the Davidson method and the Broyden charge-density mixing method were used. The structure optimization was quenched using molecular dynamics.

Synthesis: Methyltriethoxysilane ($CH_3Si(OC_2H_5)_3$), ethyltriethoxysilane ($C_2H_5Si(OC_2H_5)_3$), propyltriethoxysilane ($C_3H_7Si(OC_2H_5)_3$), and octyltriethoxysilane ($C_8H_{17}Si(OC_2H_5)_3$) were used as precursors for the formation of organosiloxane networks, and tetraethoxysilane ($Si(OC_2H_5)_4$) was used as a precursor for the formation of siloxane networks. Niobium ethoxide ($Nb(OC_2H_5)_5$), titanium isopropoxide ($Ti(O^iC_3H_7)_4$), aluminum *sec*-butoxide ($Al(O^sC_4H_9)_3$), yttrium isopropoxide ($Y(O^iC_3H_7)_3$), calcium ethoxide ($Ca(OC_2H_5)_2$), and lithium ethoxide ($LiOC_2H_5$) were used as precursors of inorganic components. Niobium ethoxide, titanium isopropoxide, aluminum *sec*-butoxide, and yttrium isopropoxide were chemically modified with ethyl acetoacetate. Ethoxysilane in 2-ethoxyethanol was partially hydrolyzed with water containing 0.1 mol % HCl in a molar ratio of 3:2 (water/ethoxysilane). Metal alkoxide was added to the partially hydrolyzed solution and stirred for 1 h. The molar ratio of aluminum *sec*-butoxide/ethoxysilane was 5:95. The solution was further hydrolyzed with an excess of water containing 0.1 mol-% HCl in a molar ratio water/(ethoxysilane + metal alkoxide) of 30:1. The hydrolyzed solution was allowed to gel at 70–100 °C for 1 day. The gel was further heat-treated at 200 °C for 1 day. The sample was ground to a powder and used for measuring the solid acid/base strength. The measurements were carried out with a series of Hammett indicators [14].

Received: October 10, 2004
Final version: May 17, 2005
Published online: September 15, 2005

[1] S. Kanzaki, M. Shimada, K. Komeya, A. Tsuge, *Key Eng. Mater.* **1999**, *437*, 161.
[2] H. Eckert, M. Ward, *Chem. Mater.* **2001**, *13*, 3059.
[3] G. Philipp, H. Schmidt, *J. Non-Cryst. Solids* **1984**, *63*, 283.
[4] J. D. MacKenzie, Y. J. Chung, Y. Hu, *J. Non-Cryst. Solids* **1992**, *147–148*, 271.
[5] D. Avnir, S. Braun, O. Lev, D. Levy, M. Ottolenghi, in *Sol–Gel Optics: Processing and Applications* (Ed: L. C. Klein), Kluwer, Dordrecht, The Netherlands **1994**, p. 539.
[6] A. Selliner, P. M. Weiss, A. Nguyen, Y. Lu, R. A. Assink, W. Gong, C. J. Brinker, *Nature* **1998**, *349*, 256.
[7] S. Inagaki, S. Guan, T. Ohsuna, O. Terasaki, *Nature* **2002**, *416*, 304.
[8] J. F. Remenar, C. J. Hawker, J. L. Hedrick, S. M. Kim, R. D. Miller, C. Nguyen, M. Trollsas, D. T. Yoon, *Mat. Res. Soc. Symp. Proc.* **1998**, *511*, 69.
[9] K. Tsuru, Y. Aburatani, T. Yabuta, S. Hayakawa, C. Ohtsuki, A. Osaka, *J. Sol-Gel Sci. Technol.* **2001**, *21*, 89.
[10] C. Noguera, *Physics and Chemistry at Oxide Surfaces*, Cambridge University Press, Cambridge, UK **1996**, p. 160.
[11] M. H. Sossina, A. B. Dane, R. I. C. Calum, B. M. Ryan, *Nature* **2001**, *410*, 910.
[12] S. Katayama, K. Iwata, Y. Kubo, N. Yamada, Y. Nonaka, *J. Appl. Phys.* **2003**, *93*, 6000.
[13] C. L. Thomas, *Ind. Eng. Chem.* **1949**, *41*, 2564.
[14] K. Tanabe, M. Misono, Y. Ono, H. Hattori, *New Solid Acids and Bases: Their Catalytic Properties*, Elsevier, Amsterdam, The Netherlands **1989**, p. 109.
[15] K. Tanabe, M. Misono, Y. Ono, H. Hattori. *New Solid Acids and Bases: Their Catalytic Properties*, Elsevier, Amsterdam, The Netherlands **1989**, p. 9.
[16] K. Cvetkovic, A. Petric, *Am. Ceram. Soc. Bull.* **2000**, *79*, 65.
[17] J.-P. Jolivet, *Metal Oxide Chemistry and Synthesis*, Wiley, New York **2000**, p. 233.
[18] P. Hohenberg, W. Kohn, *Phys. Rev. B* **1964**, *136*, 864.
[19] W. Kohn, L. J. Sham, *Phys. Rev. A* **1965**, *140*, 1133.
[20] J. P. Perdew, K. Burke, M. Ernzerhof, *Phys. Rev. Lett.* **1996**, *77*, 3865.
[21] D. Vanderdilt, *Phys. Rev. B: Condens. Matter Mater. Phys.* **1990**, *41*, 7892.
[22] N. Troullier, J. L. Martins, *Phys. Rev. B: Condens. Matter Mater. Phys.* **1991**, *43*, 1993.

Combinatorial Material Mechanics: High-Throughput Polymer Synthesis and Nanomechanical Screening**

By *Catherine A. Tweedie*, *Daniel G. Anderson*, *Robert Langer*, and *Krystyn J. Van Vliet**

Combinatorial materials science, an experimental concept developed in the 1960s for alloy development, has resurged via advances in materials synthesis.[1] Application of high-throughput syntheses toward the rapid discovery and optimization of functional materials has required parallel advances in materials characterization.[2] In the context of polymer design for applications ranging from biomaterials to microelectronic insulators, combinatorial approaches can enable systematic, high-throughput surveying of structure–processing–property relationships as a function of composition and operating conditions, in nanoliter to microliter volumes.[3–5] Here, we develop a high-throughput synthesis/nanomechanical-profiling approach capable of accurately screening the mechanical properties of a large, discrete polymer library comprising nanoliter-scale material volumes. Within just a few days, a library of over 1700 photopolymerizable materials was synthesized and then assayed for mechanical properties using

[*] Prof. K. J. Van Vliet, C. A. Tweedie
Department of Materials Science and Engineering
Massachusetts Institute of Technology
77 Massachusetts Avenue, Cambridge, MA 02139 (USA)
E-mail: krystyn@mit.edu
Dr. D. G. Anderson, Prof. R. Langer
Department of Chemical Engineering
Massachusetts Institute of Technology
77 Massachusetts Avenue, Cambridge, MA 02139 (USA)

[**] The authors thank Drs. J. F. Smith and S. Goodes of MicroMaterials, Limited for assistance with software modifications of the nanoindenter employed herein, as well as M. J. Cima for helpful discussion and constructive criticism. C. A. T. gratefully acknowledges support through the National Defense Science and Engineering Graduate Fellowship program. D. G. A. and R. L. acknowledge support from NIH grant #RO1DE016516-01 and 4.1 Switchable Surfaces by the U.S. Army Research Office (contract #DAAD-19-02D002) through the Institute for Soldier Nanotechnologies at MIT. The content of the information does not necessarily reflect the position or the policy of the Government, and no official endorsement should be inferred.

 DOI: 10.1002/adma.200501142

ADVANCED MATERIALS

an automated nanomechanical screening system. The approach outlined herein enables the rapid correlation of polymer composition, processing, and structure with mechanical performance metrics.

Efficient and accurate quantification of the mechanical behavior of materials is of broad significance to material discovery, characterization, and model validation. In fact, the mechanical properties of small material volumes (nm^3–μm^3) are increasingly important aspects of performance in non-structural contexts ranging from low-dielectric-constant (low-κ) thin films and metal interconnect lines in microelectronics[6] to abrasion-resistant palliative coatings,[7] photonics-compatible adhesives,[8] and polymeric biomaterials.[5,9,10] Conventional materials development and characterization—the serial process of bulk-material synthesis, batch-sample preparation, and individual-sample testing (e.g., uniaxial tensile testing of several material coupons machined to a specific geometry)—typically occurs over the span of weeks to months. Parallelization of this effort through combinatorial approaches has the potential to not only screen a large number of materials more efficiently, but also to enable material design through systematic variation in composition, processing, and/or microstructure.[11] Thus, we sought to develop an accurate, high-throughput analysis of relevant mechanical properties of polymers, facilitating subsequent correlation of these properties with material composition and functional performance.

To maximize throughput and mechanical-property accuracy while minimizing reagent cost, we considered a discrete polymer library as a microarray format of nanoliter-scale material volumes. While combinatorial biomolecular libraries such as DNA microarrays are commonly used, the synthesis of discrete polymer libraries—an array of micrometer-scale spots, each representing a stepwise change in composition and/or processing of crosslinked molecules—has been a challenge.[4,12] This is due to both polymer physics, in that monomers deposited in solution must polymerize and crosslink within the small reaction volume of the droplet, and technical challenges such as reliable printing of high viscosity (high-molecular-weight) solutions. Anderson et al.[13] have recently demonstrated this capability in the context of a wide range of acrylate-based crosslinked polymers printed onto glass slides (Fig. 1). Semiquantitative mechanical characteristics of temperature- and composition-gradient polymer libraries have been assessed via pointwise, microscale impact testing of polymer films peeled from deposition substrates, to correlate processing history of a small subset of the gradient library with impact energy and failure modes.[14] However, for reasons related to solution-based materials synthesis, accurate interpretation of nanomechanical experiments, and application-specific assays of material performance, discrete polymer libraries such as in Figure 1 are often preferable to continuous gradient libraries.[3,15]

Nanoindentation, a continuous measurement of load versus nanometer-scale displacement of a rigid indenter into a material surface, has been proposed as an experimental approach particularly well suited to rapid mechanical characterization of the small representative volume elements (RVEs) of gradient or discrete material libraries.[1,3] From the load–displacement (P–h) hysteretic response of the RVE (Fig. 2), bulk mechanical properties, including elastic modulus E and semi-quantitative mechanical parameters such as hardness H, can be estimated in closed form.[16–19] As nanoindentation inherently probes cubic nanometer to cubic micrometer material

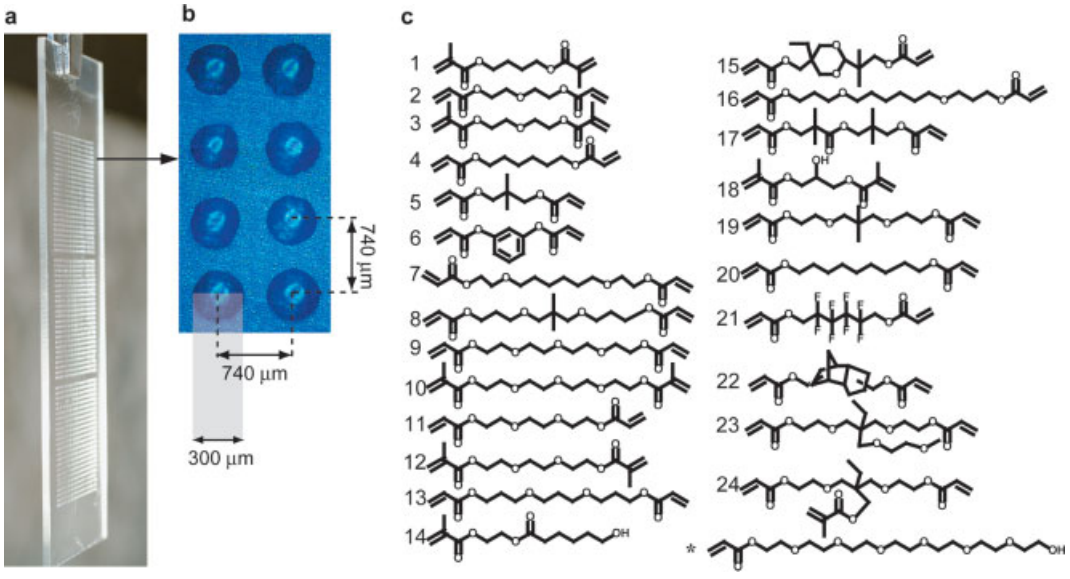

Figure 1. Discrete polymer library. a) Pairwise combinations of 24 monomers printed as 576-spot arrays in triplicate on standard glass slide. b) Differential interference contrast image shows spots of 300 µm diameter and 15 µm thickness/5 Å root-mean-square surface roughness are located in square arrays of 740 µm center-to-center spacing. c) Monomer structure notation; monoacrylate (*) was added at 30 vol.-% instead of monomer 17 to increase hydrophilicity.

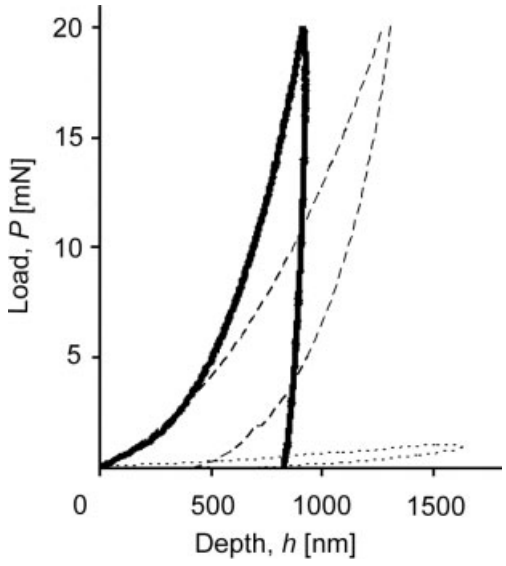

Figure 2. Representative nanoindentation load–displacement responses. Comparative responses of borosilicate glass (solid line); a stiff polymer spot in the array (70% monomer 19: 30% monomer 24, dashed line); and the most compliant polymer spot in the array (70% monomer 11: 30% monomer 8, dotted line). Area circumscribed by the hysteresis quantifies energy absorbed by the polymer. Maximum depth for the most compliant polymer was 1800 nm, or 12% of spot thickness. Profilometry indicates a spot radius of curvature ρ of approximately 1270 μm and thickness of approximately 15 μm, indicating that indentations near the spot center would be < 10% spot thickness t on a surface with no more than 3° relative tilt.

volumes, it is theoretically possible to mitigate the contributions of adjacent material by restricting the maximum depth of indentation h_{max} to be much less than the RVE diameter and thickness, or to separate these contributions by semi-analytical deconvolution of the responses of the RVE and adjacent material. This is a particularly important consideration in nanoindentation characterization of thin films, for which instrumented nanoindentation was originally developed, and has been addressed by several researchers. In fact, nanoindentation has been applied recently to the analysis of gradient libraries of metal-alloy thin films: large circular metal films in which the composition is changed continuously as a function of radial distance.[15,20] Technology required to apply this approach to rapid and accurate analysis of large polymer libraries—which, unlike metals, exhibit large displacements under small applied loads—requires unique considerations (see Experimental). If the rigid indenter geometry can be approximated as a sharp cone and the indented material can be approximated as a linear elastic–plastic solid, then:

$$E_r = \beta \, dP/dh \mid_{P\max} / (A_{max})^{1/2} \quad (1)$$

$$H = P_{max}/A_{max} \quad (2)$$

where E_r is the reduced elastic modulus of both the indenter and sample materials, β is a geometrical constant related to the apex angle of the indenter, and A_{max} is the maximum projected indentation contact area which can be calculated from the nanoindentation data as a function of h:[18,21] $A_{max} = 24.5\, h_{max}^2$ assuming ideal geometry of the Berkovich (trigonal pyramid) indenter used herein. The sample elastic modulus E_s can be determined directly as:

$$E_r = [(1-\nu_i^2)/E_i + (1-\nu_s^2)/E_s]^{-1} \quad (3)$$

where E_i and ν_i of the diamond indenter are 1100 GPa and 0.07, respectively, and ν_s of the polymer samples is assumed as 0.45. Thus, the applied stress state and calculation of mechanical properties from these data are well defined and validated by applications unrelated to combinatorial materials research.[18,22,23] More complex analyses relate the dynamic P–h response to mechanical properties of time-dependent materials such as polymers, although it has been demonstrated that many polymers do not conform to the assumptions of linear viscoelasticity inherent in these analyses.[23,24]

Here, a large array of 1728 distinct polymer spots was synthesized and then analyzed via nanoindentation. In order to determine precision and accuracy of this approach, each sample included arrays printed in triplicate: each of the three arrays comprised 576 unique polymers, arranged in 24 subarrays each comprising 24 polymer spots representing all possible pairwise combinations of 70 vol.-% major monomer/30 vol.-% minor monomer. Polymer spots were ~300 μm in diameter and ~15 μm in thickness, t_p, with 740 μm center-to-center spacing (Fig. 1). The monomer structures are shown in Figure 1c.

The triplicate array (1728 polymer spots) was printed on a standard glass slide in less than 24 h via a modified robotic fluid-handling system. Upon automated calibration of nanoindenter (MicroMaterials Limited, Wrexham, UK) load and depth transducers (as a function of signal voltages) and readily implemented modifications of translational-stage displacement maxima and interindentation delay, the entire array (representing 576 unique polymer compositions) was mechanically characterized in 24 h of continuous, automated acquisition and analysis of nanoindentation P–h responses (Fig. 2), with maximum indentation depths $h_{max} = 1.5$ μm (~10% t_p) as shown for one of the three arrays in Figure 3. As the array was regularly spaced, automated data acquisition required simply that the first indentation occurred near the center of any spot in a subarray, which could be achieved visually or via profilometric scanning across a polymer spot with the indenter. To establish precision of the approach as well as material uniformity, adjacent subarrays of major monomers **1**, **2**, **5**, and **6**, each with 24 individual polymer spots, were nanoindented on each of the triplicate arrays. Under the loading rate and stage-displacement rates implemented, a single subarray could be automatically nanoindented and analyzed for E and H in about 1 h, such that the entire array could be completely and automatically analyzed in a 24 h cycle. Although cycle time could be decreased considerably and easily through more rapid sample actuation and/or increased loading rates,

ADVANCED MATERIALS

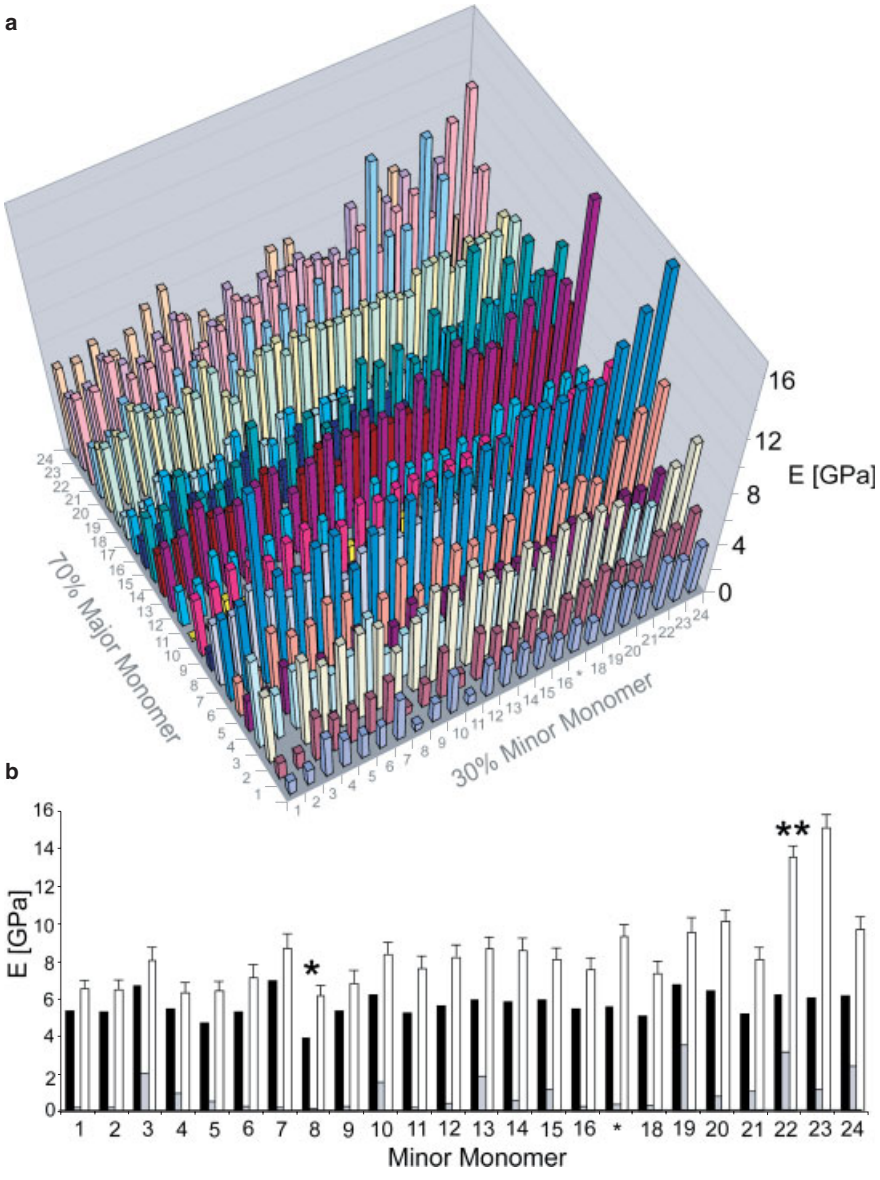

Figure 3. Automated array-nanoindentation determination of elastic modulus *E* for entire 576-element polymer library. a) Nanoindentation data were acquired and analyzed in 24 h of instrument time, with high precision and accuracy. b) Subarrays of major monomer 8 (black); major monomer 11 (gray); and major monomer 22 (white). Error bars represent the maximum observed standard deviation of 7.5 % among the triplicate subarrays (shown only on major monomer 22 data for clarity). Large asterisks depict polymer spots of minimum *E* (30 % monomer 8) and maximum *E* (30 % monomer 19 or 22) within a given subarray. Values of *E* are comparable to the range for macroscopic, crosslinked polymers characterized by uniaxial testing [25].

the nanoindentation analysis employed herein assumes quasistatic loading. This approach is experimentally and analytically simpler to implement than dynamic loading methods that idealize the polymer as a configuration of springs and dashpots, which is an important consideration for robust combinatorial approaches. However, Kossuth et al. have implemented simplifying assumptions to achieve parallel dynamic testing of small, discrete polymer composite libraries (96 sample films of microliter-scale volumes and millimeter-scale diameter on a flexible polyimide substrate) with reasonable repeatability of estimated complex modulus E_c over different temperatures (standard deviation/mean ranging 11 %–125 % for identical polystyrene samples). The speed of this testing was not reported.[26]

Representative results for *E* for the entire array (576 spots) and a key subset are shown in Figure 3. Several trends are immediately apparent. First, *E* measured for any particular major monomer is not strongly affected by the addition of a minor monomer. That is, the standard deviation of the average *E* in a subarray comprising a given major monomer is typically <2 GPa, regardless of minor-monomer structure. Thus, although the minor-monomer structure clearly modulates *E* of the copolymer in a consistent fashion, in general, the major monomer more strongly influences copolymer stiffness. Secondly, certain minor monomers significantly and consistently affect *E* within this library. Specifically, when monomers **8** and **11** are the minor components (30 vol.-%), the resulting copolymers are the most compliant observed within any given major monomer subarray (Fig. 3b). Thirdly, the mechanical properties of a copolymer are not necessarily consistent with those of the bulk counterparts. In fact, although polymers with 30 vol.-% monomer **8** were identified as the most compliant polymers in 92 % of the subarrays, the subarray comprising 70 vol.-% monomer **8** exhibited an average $E = 5.7 \pm 0.7$ GPa, ranking 12th in compliance among the 24 major monomer combinations. In contrast, polymers comprising a major volume fraction of monomer **11** (70 vol.-%) resulted in the most compliant subarray of the 24 considered. This finding, which would not be expected solely from consideration of monomer structure and volume fraction, indicates that there is a critical volume fraction of monomer **8**, beyond which there exists a microstructural and/or phase change concomitant with a significant increase in mechanical stiffness.

Importantly, the error bars in Figure 3b represent the standard deviation among the triplicate arrays—incidentally acquired on three separate days—and are not greater than 10 % for any specific polymer spot. This level of repeatability is

comparable to the standard deviation observed for an array of nanoindentations on a single, bulk metal sample of homogenous microstructure.[27] This underscores the high reliability of the discrete polymer library deposition approach, as well as the precision of the nanoindentation approach used herein.[28] Further, the accuracy of this approach is demonstrated by analysis of the nanoindentation response of the glass slide. A series of experiments was conducted in which the interindentation spacing was decreased by a factor of two, such that polymer spots and the glass slide were nanoindented alternately. From these data it was found that $E_{glass} = 67 \pm 2$ GPa, which is consistent with bulk measurements of E_r for borosilicate glass.[29,30] Finally, a small subset of polymer spots was indented to two different h_{max} (1 and 1.5 μm) at the same loading rate of 2 mN s^{-1}, and the calculated E was found to vary no more than 6.5 % as a function of maximum depth/applied load.

In summary, automated array synthesis and indentation analysis provides a general, rapid, precise, and accurate mechanical characterization of discrete material libraries. Automated analysis of a large library of acrylate-based materials demonstrates a range of mechanical properties that are affected by polymer composition in unexpected ways. These studies provide the first large-scale analysis of structure–property relationships governing the mechanical response of combinatorial, acrylate-based materials. These methods are suitable for the analysis of crosslinked polymers for functional applications such as biological substrata, enabling studies of mechanical cues on cell behavior.[10,31] Likewise, this approach can be applied to the discovery of new materials that require dual optimization of mechanical and other functional properties, such as environmentally inert structural coatings and insulating films in microelectronics. Beyond the immediate utility of material screening and discovery, the experimental capability demonstrated herein could accelerate the development of accurate material models relating monomer structure, microstructure, and mechanical response.

Experimental

Combinatorial Array Preparation: Polymers were printed in a humid Ar-atmosphere on epoxy monolayer-coated glass slides (Xenopore XENOSLIDE E, Hawthorne, NJ [32]) which were first dip-coated in 4 vol.-% pHEMA (pHEMA = poly(hydroxyethyl methacrylate)), using modifications of robotic fluid-handling technology as described previously [3]. Spots were polymerized via ~10 s exposure to long-wave UV, and dried at <50 mtorr (1 torr = 133.32 Pa) for at least 7 days prior to nanoindentation array analysis.

Nanoindentation: Nanoindentation experiments were conducted on a pendulum-based nanoindenter equipped with a scanning stage (NanoTest600 NT1, MicroMaterials, Wrexham, UK), and fitted with a diamond Berkovich indenter (trigonal pyramid of apex semiangle ~71°). This instrument has force and displacement resolution of 1.5 μN and better than 0.1 nm, respectively, and force and displacement maxima of 30 mN and 4 μm, respectively. Automated calibration of load and depth transducers requires <1 h. All indentations proceeded in load control at a rate of 2 mN s^{-1} to a maximum depth of 1.5 μm (or 20 mN, whichever was attained first; the latter condition was attained only for nanoindentations on glass and the stiffest polymers). Positioning of the indenter on the center of the first polymer spot on the array was refined by isoforce profiling of the spot topography via the x–y scanning stage. This approach is similar to scanning probe microscopy, but uses the relatively blunt indenter (radius ~100 nm) as the scanning probe. Additionally, conventional profilometry (Tencor P10 Surface Prolifometer, San Jose, CA) was used to determine the average radius of curvature ρ and height t of spots ($\rho_{avg} = 1269$ μm; $t_{avg} = 17$ μm). An array of nanoindentations was programmed via stage translation, based on the polymer library spacing (740 μm inter-indentation spacing). Load–depth indentation data were analyzed for E and H via the method of Oliver and Pharr [18], which neglects material viscoelasticity and/or pile-up of the indented material, where the unloading portion of the data was analyzed to obtain $dP/dh|_{P_{max}}$ by fitting the conventional power law form from $0.90\,P_{max}$ to $0.20\,P_{max}$.

Although nanoindentation is an increasingly automated experiment that is possible using instrumentation ranging from commercial machines to home-built atomic force microscopes, application of this approach for combinatorial materials science—particularly in discrete polymer libraries—requires unique considerations. First, the instrument must include a sample translation stage that facilitates rapid motion among array positions, as well as sufficient load and displacement resolution/maxima to reliably contact relatively soft materials. Secondly, both the load/displacement transducers and the sample translation stage should be stable against thermal/electronic drift, so that no post-test data correction is required and so that every element in the combinatorial array is accessed with high positional accuracy. The absence of piezocrystal-actuation in the load frame of the indenter used herein resulted in frame compliance and load/displacement signals that were extremely stable and repeatable. Third, in experiments different from those that consider microstructurally heterogeneous polymers (e.g., crystalline domains in an amorphous matrix), the maximum indentation volume will dictate whether the calculated properties represent the composite or minor-phase response. Although the solution is not straightforward or general, it is advisable to restrict indentation depths to < 1/10 of the minor-phase diameter (typically via sharp geometries) to capture this response, and at least 10 times the minor-phase diameter (typically via blunt/spherical geometries) to capture the composite mechanical response of the material.

Received: June 6, 2005
Final version: August 17, 2005
Published online: September 29, 2005

[1] E. J. Amis, X. D. Xiang, J. C. Zhao, *MRS Bull.* **2002**, *27*, 295.
[2] S. Schmatloch, U. S. Schubert, *Macromol. Rapid Commun.* **2004**, *25*, 69.
[3] J. C. Meredith, A. Karim, E. J. Amis, *MRS Bull.* **2002**, *27*, 330.
[4] M. P. Stoykovich, H. B. Cao, K. Yoshimoto, L. E. Ocola, P. F. Nealey, *Adv. Mater.* **2003**, *15*, 1180.
[5] D. G. Anderson, D. Putnam, E. B. Lavik, T. A. Mahmood, R. Langer, *Biomaterials* **2005**, *26*, 4892.
[6] Y. Choi, K. J. Van Vliet, S. Suresh, *J. Appl. Phys.* **2003**, *94*, 6050.
[7] C. M. Chan, G. Z. Cao, H. Fong, M. Sarikaya, T. Robinson, L. Nelson, *J. Mater. Res.* **2000**, *15*, 148.
[8] B. G. Yacobi, S. Martin, K. Davis, A. Hudson, M. Hubert, *J. Appl. Phys.* **2002**, *91*, 6227.
[9] A. J. Engler, L. Richert, J. Y. Wong, C. Picart, D. E. Discher, *Surf. Sci.* **2004**, *570*, 142.
[10] M. Thompson, M. Berg, I. Tobias, M. Rubner, K. J. Van Vliet, *Biomaterials* **2005**, *26*, 6836.
[11] M. A. R. Meier, U. S. Schubert, *J. Mater. Chem.* **2004**, *14*, 3289.
[12] A. Leugers, D. R. Neithamer, L. S. Sun, J. E. Hetzner, S. Hilty, S. Hong, M. Krause, K. Beyerlein, *J. Comb. Chem.* **2003**, *5*, 238.

ADVANCED MATERIALS

[13] D. G. Anderson, S. Levenberg, R. Langer, *Nat. Biotechnol.* **2004**, *22*, 863.
[14] J.-L. Sormana, J. C. Meredith, *Macromol. Rapid Commun.* **2003**, *24*, 118.
[15] S. M. Han, R. Shah, R. Banerjee, G. B. Viswanathan, B. M. Clemens, W. D. Nix, *Acta Mater.* **2005**, *53*, 2059.
[16] A. E. Giannakopoulos, S. Suresh, *Scr. Mater.* **1999**, *40*, 1191.
[17] M. Dao, N. Chollacoop, K. J. Van Vliet, T. A. Venkatesh, S. Suresh, *Acta Mater.* **2001**, *49*, 3899.
[18] W. C. Oliver, G. M. Pharr, *J. Mater. Res.* **1992**, *7*, 1564.
[19] M. F. Doerner, W. D. Nix, *J. Mater. Res.* **1986**, *1*, 601.
[20] A. Rar, J. J. Frafjord, J. D. Fowlkes, E. D. Specht, P. D. Rack, M. L. Santella, H. Bei, E. P. George, G. M. Pharr, *Meas. Sci. Technol.* **2005**, *16*, 46.
[21] I. N. Sneddon, *Int. J. Eng. Sci.* **1965**, *3*, 47.
[22] K. J. Van Vliet, J. Li, T. Zhu, S. Yip, S. Suresh, *Phys. Rev. B* **2003**, *67*, 104 105.
[23] M. R. VanLandingham, J. S. Villarrubia, W. F. Guthrie, G. F. Meyers, *Macromol. Symp.* **2001**, *167*, 15.
[24] C. A. Tweedie, J. F. Smith, K. J. Van Vliet, in *Materials Research Society Fall Symposium*, Vol. 841 (Eds: N. H. K. J. Wahl, A. B. Mann, D. F. Bahr, Y.-T. Cheng), Materials Research Society, Boston, MA **2004**.
[25] M. Ashby, *Materials Selection in Mechanical Design*, Butterworth-Heineman, Oxford **1999**.
[26] M. B. Kossuth, D. A. Hajduk, C. Freitag, J. Varni, *Macromol. Rapid Commun.* **2004**, *25*, 243.
[27] K. J. Van Vliet, L. Prchlik, J. F. Smith, *J. Mater. Res.* **2004**, *19*, 325.
[28] Calculated values of H showed similar trends and repeatability (<8% standard deviation among triplicates), but data are not shown, since hardness—the resistance of a material to permanent deformation as quantified by Equation 2—is not a true mechanical property, is a poor metric of mechanical behavior in time-dependent materials such as polymers [19], and is not particularly relevant to the present application of this polymer library.
[29] http://www.matweb.com/search/SpecificMaterial.asp?bassnum=BGLAS0, accessed June 2005.
[30] http://www.sas.org/E-Bulletin/archive/reference/material/byMaterial.html, accessed June 2005.
[31] A. Shukla, A. R. Dunn, M. A. Moses, K. J. Van Vliet, *Mech. Chem. Biosyst.* **2004**, *4*, 279.
[32] Xenopore. http://www.xenopore.com/Microarray%20Products.htm, accessed June 2005.

Surface-Nucleated Assembly of Fibrillar Extracellular Matrices**

By *Jeffrey R. Capadona*, *Timothy A. Petrie*, *Kenan P. Fears*, *Robert A. Latour*, *David M. Collard*, and *Andrés J. García**

Extracellular matrices (ECMs), comprised of insoluble networks of proteins and polysaccharides, regulate cellular activities to direct the formation, maintenance, and repair of numerous tissues.[1,2] While nanostructured and synthetic substrates incorporating biological motifs, such as adhesion and growth-factor binding sites, have been generated,[3,4] these materials exhibit reduced bioactivity compared to natural biopolymers. In particular, the inability of synthetic materials to reconstitute the higher order, supramolecular structure of native ECMs limits the development of bio-interactive materials for regenerative medicine. A vital property of ECMs is the fibrillar architecture arising from supramolecular assembly. For example, the fibrillar structure of fibronectin (FN) matrices modulates cell cycle progression, migration, gene expression, cell differentiation, and the assembly of other matrix proteins.[5–11] While most cell types can deposit ECMs on synthetic materials, current biomaterials do not actively direct deposition and assembly of fibrillar, supramolecular structures characteristic of natural matrices. By covalently immobilizing an oligopeptide (FN13) from the self-assembly domain of fibronectin,[5] we have engineered surfaces that nucleate the assembly of robust fibrillar FN matrices. FN13-nucleated FN matrices template the assembly of collagen (COL) fibrils within the FN architecture and exhibit higher cell proliferation rates. These synthetic substrates provide a promising route to direct the assembly of supramolecular matrices for enhanced cellular responses.

In the present study, oligopeptides, including FN13 (KGGGAHEEICTTNEGVM), bioadhesive RGD (GRGDSPC), and control-scrambled sequences (KGGGITCETNEGEVAMH), were selectively tethered onto self-as-

[*] Dr. A. J. García, Dr. J. R. Capadona, T. A. Petrie
Petit Institute for Bioengineering and Bioscience
Georgia Institute of Technology, Atlanta, GA 30332 (USA)
E-mail: andres.garcia@me.gatech.edu
Dr. A. J. García, T. A. Petrie
Woodruff School of Mechanical Engineering
Georgia Institute of Technology, Atlanta, GA 30332 (USA)
Dr. J. R. Capadona, Dr. D. M. Collard
School of Chemistry and Biochemistry
Georgia Institute of Technology
Atlanta, GA 30332 (USA)
K. P. Fears, Dr. R. A. Latour
Department of Bioengineering, Clemson University
Clemson, SC 29634 (USA)

[**] This work was funded by NSF CAREER (BES-0093226) and the Georgia Tech/Emory NSF ERC on the Engineering of Living Tissues (EEC-9731643). The authors thank J. L. Charest and W. P. King for micropatterning stamps. Supporting Information is available online from Wiley InterScience or from the author.

  DOI: 10.1002/adma.200500959